ELSEVIER

Journal of Organometallic Chemistry 659 (2002) 73–83

Journal of Organometallic Chemistry

www.elsevier.com/locate/jorganchem

A novel route for the preparation of dimeric tetraorganodistannoxanes

Jens Beckmann [a], Dainis Dakternieks [a,*], Fong Sheen Kuan [a], Edward R.T. Tiekink [b,*]

[a] *Centre for Chiral and Molecular Technologies, Deakin University, Geelong, Vic. 3217, Australia*
[b] *Department of Chemistry, The University of Adelaide, Adelaide, SA 5005, Australia*

Received 30 May 2002; received in revised form 1 July 2002; accepted 1 July 2002

Abstract

The reaction of polymeric diorganotin oxides, $(R_2SnO)_n$ (R = Me, Et, *n*-Bu, *n*-Oct, *c*-Hex, *i*-Pr, Ph), with saturated aqueous NH_4X (X = F, Cl, Br, I, OAc) in refluxing 1,4-dioxane afforded in high yields dimeric tetraorganodistannoxanes, $[R_2(X)SnOSn(X)R_2]_2$, and in a few cases diorganotin dihalides or diacetates, R_2SnX_2. The reported method appears suitable for the synthesis of fluorinated tetraorganodistannoxanes. Identification of $[R_2(OH)SnOSn(X)R_2]_2$ (R = *n*-Bu; X = Cl, Br) and $[R_2(OH)SnOSn(X)R_2]$ $[R_2(X)SnOSn(X)R_2]$ suggest a serial substitution mechanism starting from $[R_2(OH)SnOSn(OH)R_2]_2$. X-ray crystal structure determinations are reported for $[Me_2(AcO)SnOSn(OAc)Me_2]_2$ (**29a**), $[i\text{-}Pr_2(Br)SnOSn(Br)i\text{-}Pr_2]_2$ (**20a**), $[c\text{-}Hex_2(F)SnOSn(F)c\text{-}Hex_2]_2$ (**5a**) and $[c\text{-}Hex_2(F)SnOSn(Cl)c\text{-}Hex_2]_2$ (**36**), respectively. These show the presence of a central $(R_2Sn)_2O_2$ core that is connected, via the oxygen atoms, to R_2Sn entities. Acetate (**29a**) or halides (**5a**, **20a, 36**) complete the coordination about the tin centres. © 2002 Elsevier Science B.V. All rights reserved.

Keywords: Tin; Tetraorganodistannoxane; ^{119}Sn-NMR spectroscopy; X-ray crystallography

1. Introduction

Tetraorganodistannoxanes with dimeric ladders structures $[R_2(X)SnOSn(Y)R'_2]_2$ (R, R′ = alkyl or aryl; X = Y = Hal, OH, OR, $OSiMe_3$, OOCR, $OSP(OR)_2$, NO_3, N_3, NCS, SH, $OReO_3$, NCO, $OB(OR)_2$, ROO, RSO_3, RS), have been widely exploited over recent years owing to their unique structural features (Scheme 1) [1–10]. They are also of interest as highly selective, homogeneous catalysts in various organic reactions such as transesterification, acylation of alcohols, urethane formation and alkyl carbonate synthesis [11–24]. More recently dimeric tetraorganodistannoxanes bearing perfluorinated substituents were used as catalysts in three liquid phase systems involving fluorinated solvents [25].

In the past, dimeric tetraorganodistannoxanes with X, Y = Hal, OH have been prepared by the partial hydrolysis of diorganotin dihalides. However, this method is not always straightforward and requires specific conditions for each product, which are for new systems unpredictable [5,26–32]. A more general approach for the synthesis of derivatives with X = Y = Hal is from a reaction between equimolar amounts of diorganotin oxide and diorganotin dihalide. A shortcoming of this method is the requirement that the diorganotin oxide must be sufficiently soluble in organic solvents [33,34]. Furthermore, this method fails to provide fluorinated tetraorganodistannoxanes, due to the insolubility of diorganotin difluorides. Consequently, only very few examples have been reported so far [35].

Earlier work showed that reaction between diorganotin oxides and ammonium halides in methylcyclohexane at reflux resulted in formation of diorganotin dihalides [36].

In the present work, we report a new and facile way of generating dimeric tetraorganodistannoxanes with X = Y = halogen using $(R_2SnO)_n$ (R = Me, Et, *n*-Bu, *n*-Oct, *c*-Hex, *i*-Pr, Ph) and a biphasic solvent mixture consisting of saturated aqueous NH_4X solution (X = F, Cl, Br, I, OAc) and 1,4-dioxane. Thus, we have been able to generate a number of already reported as well as some

---

* Corresponding authors. Present address: Department of Chemistry, National University of Singapore, Singapore 117543, Singapore (E.R.T.T.). E-mail sddress: chtert@nus.edu.sg

E-mail address: dainis@mail.deakin.edu.au (D. Dakternieks).

0022-328X/02/$ - see front matter © 2002 Elsevier Science B.V. All rights reserved.
PII: S0022-328X(02)01705-9

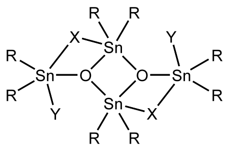

R = alkyl, aryl; X, Y = Hal, OH, OR, $OSiMe_3$, OOCR, $OSP(OR)_2$, NO_3, N_3, NCS, SH, $OReO_3$, NCO, $OB(OR)_2$, ROO, RSO_3, RS

Scheme 1.

hitherto unknown dimeric tetraorganodistannoxanes. Compounds were characterised by ^{119}Sn-NMR spectroscopy in solution and in the solid state and in some representative cases by X-ray crystallography.

2. Results and discussion

2.1. Synthetic aspects

The reaction of the diorganotin oxides, $(R_2SnO)_n$ (R = Me, Et, *n*-Bu, *n*-Oct, *c*-Hex, *i*-Pr, Ph), with aqueous NH_4X (X = Hal, OAc) was performed in refluxing dioxane (Eq. (1)). The reactions were usually complete when all of the polymeric diorganotin oxide had dissolved (12–96 h). In most cases pure dimeric tetraorganodistannoxane, $[R_2(X)SnOSn(X)R_2]_2$ (hereafter denoted with ‘a’) were obtained after standard work-up and in few cases diorganotin dihalides or diacetates, R_2SnX_2 (hereafter denoted with ‘b’), were obtained in good to high yields. Detailed results are presented in Table 1 and are discussed below.

$$(R_2SnO)_n + NH_4X \xrightarrow[\text{reflux, 12-96 h}]{\text{1,4-dioxane}} \underset{\mathbf{a}}{[R_2(X)SnOSn(X)R_2]_2} + \underset{\mathbf{b}}{R_2SnX_2} \qquad (1)$$

R = Me, Et, *n*-Bu, *n*-Oct, *i*-Pr, *c*-Hex, Ph
X = Hal, OAc

2.1.1. Reactions of $(R_2SnO)_n$ with NH_4F

The reaction of $(R_2SnO)_n$ with NH_4F afforded dimeric tetraorganodistannoxanes $[R_2(F)SnOSn(F)R_2]_2$ (R = *n*-Bu (**3a**) [37], *c*-Hex (**5a**)). However, for R = Me, Et, *n*-Oct, *i*-Pr and Ph only inseparable mixtures were obtained. Moreover, for R = Me, Et and Ph the low yield of these mixtures suggests that substantial amounts of organotin species were not extracted from the aqueous layers. This observation might be tentatively attributed to the formation of charged organotin species, such as $[R_2SnF_3]^-$, $[(R_2SnF_2)_2F]^-$ and $[R_2SnF_4]^{2-}$ [38,39]. For R = *n*-Oct and *i*-Pr the ^{119}Sn-NMR spectra of the crude mixtures revealed 12 and 17 signals, respectively, in the region between −15 and −190 ppm.

In $CDCl_3$ solution, $[n\text{-}Bu_2(F)SnOSn(F)n\text{-}Bu_2]_2$ (**3a**) and $[c\text{-}Hex_2(F)SnOSn(F)c\text{-}Hex_2]_2$ (**5a**) are unambiguously characterised by ^{119}Sn-NMR spectroscopy, which reveals for each compound two triplets centred at −142.2 ($^1J(^{119}Sn-^{19}F) = 771$ Hz) and −159.4 ppm ($^1J(^{119}Sn-^{19}F) = 1795$ Hz) for **3a** and at −237.6 ($^1J(^{119}Sn-^{19}F) = 1950$ Hz) and −212.0 ppm ($^1J(^{119}Sn-^{19}F) = 783$ Hz) for **5a**. The observation of well-resolved triplets for **3a** contradicts the results of Jain et al. who reported a broad signal at −156 ppm for this compound [37].

2.1.2. Reactions of $(R_2SnO)_n$ with NH_4Cl

The reaction of $(R_2SnO)_n$ with NH_4Cl provided dimeric tetraorganodistannoxanes $[R_2(Cl)SnOSn(Cl)R_2]_2$ (R = Me (**8a**) [4], Et (**9a**) [4], *n*-Bu (**10a**) [4], *n*-Oct (**11a**), *c*-Hex (**12a**)) and diorganotin dichlorides R_2SnCl_2 (R = *i*-Pr (**13b**) [40], Ph (**14b**) [41]), respectively. In view of the fact that *c*-Hex groups are bulkier than Ph groups, the formation of **12a** and **14b** suggests that not only the steric demand of the substituents, but also the group electronegativities of the substituents determines the favoured product of the reactions.

The course of reaction between $(n\text{-}Bu_2SnO)_n$ and NH_4Cl was monitored using ^{119}Sn-NMR spectroscopy. A representative sample was taken after 24 h (total reaction time 48 h), the ^{119}Sn-NMR spectrum ($CDCl_3$) of which revealed eight signals between −80 and −190 ppm (Fig. 1). The connectivity of these signals was established by 1D and 2D INADEQUATE ^{119}Sn-NMR spectroscopy. Accordingly, the signals were unambiguously assigned to $[n\text{-}Bu_2(OH)SnOSn(Cl)n\text{-}Bu_2]_2$ (**10d**, δ (^{119}Sn): −138.8, −159.8; total integral 12%) [42], $[n\text{-}Bu_2(OH)SnOSn(Cl)n\text{-}Bu_2][n\text{-}Bu_2(Cl)SnOSn(Cl)n\text{-}Bu_2]$ (**10c**, δ (^{119}Sn): −93.4, −125.6, −132.2, −175.2; total integral 61%), and $[n\text{-}Bu_2(Cl)SnOSn(Cl)n\text{-}Bu_2]_2$ (**10a**, δ (^{119}Sn): −90.7, −139.1; total integral 27%) [42]. The coexistence of the latter three tetraorganodistannoxanes demonstrates that the redistribution reaction between these species is slow on the ^{119}Sn-NMR time scale [43]. It also suggests that the reaction mechanism appears to involve the initial formation of tetrahydroxide species $[n\text{-}Bu_2(OH)SnOSn(OH)n\text{-}Bu_2]_2$ from which hydroxides are replaced in a stepwise fashion by chlorides.

2.1.3. Reactions of $(R_2SnO)_n$ with NH_4Br

The reaction of $(R_2SnO)_n$ with NH_4Br produced tetraorganodistannoxanes $[R_2(Br)SnOSn(Br)R_2]_2$ (R = Et (**16a**) [3], *n*-Bu (**17a**) [3], *n*-Oct (**18a**), *i*-Pr (**20a**)) and diorganotin dibromides R_2SnBr_2 (R = *c*-Hex (**19b**) [44], Ph (**21b**) [41]), respectively. The reaction of $(Me_2SnO)_n$ with NH_4Br provided a mixture of unknown products, which could not be separated. The ^{119}Sn-NMR ($CDCl_3$) spectrum of this mixture revealed 12 signals between −131.5 and −153.5 ppm, which were tentatively assigned to pentacoordinate tin atoms.

The course of reaction between $(n\text{-}Bu_2SnO)_n$ and NH_4Br was also monitored using ^{119}Sn-NMR spectroscopy. A representative sample was taken after 24 h

Table 1
Details for the preparation of dimeric tetraorganodistannoxanes ('**a**') and diorganotin dihalides or diacetates ('**b**')

Entry	NH_4X	$(R_2SnO)_n$	Time (h)	Product(s)	Yield (%)	Melting point (°C)	δ (^{119}Sn) (ppm)
1	F	Me	48	Complex mixture [a]	.		
2		Et	24	Complex mixture [b]			
3		*n*-Bu	48	**3a**	75	115–117	−142.2, −159.4
4		*n*-Oct	48	Complex mixture [c]			
5		*c*-Hex	48	**5a**	86	> 295 (dec.)	−212.0, −237.6
6		*i*-Pr	20	Complex mixture [d]			
7		Ph	12	Complex mixture [e]		> 310 (dec.)	
8	Cl	Me	48	**8a**	82	> 280	−62.6, −114.4
9		Et	24	**9a**	60	168–170	−89.1, −137.6 [g]
10		*n*-Bu	48	**10a**	96	110–111	−91.4, −140.3
11		*n*-Oct	48	**11a**	92	94–95	−90.8, −138.2
12		*c*-Hex	24	**12a**	84	> 250 (dec.)	−139.0, −202.7
13		*i*-Pr	20	**13b**	92	80–84	83.5
14		Ph	12	**14b**	95	41–42	−53.5
15	Br	Me	48	Complex mixture [f]		74–76	
16		Et	24	**16a**	60	176–178	−79.3, −128.9 [h]
17		*n*-Bu	48	**17a**	95	103–104	−81.3, −129.8
18		*n*-Oct	48	**18a**	90	63–64	−82.0, −130.1
19		*c*-Hex	24	**19b**	90	58–59	62.3
20		*i*-Pr	24	**20a**	80	> 270 (dec.)	−91.9, −144.0
21		Ph	12	**21b**	92	110–114	−81.8
22	I	Me	48	**22b**	62	41–43	−159
23		Et	24	Complex mixture [i]			
24		*n*-Bu	60	**24a**	60	120–125	−169.7, −173.9
25		*n*-Oct	48	**25a**	80	90–95	−169.9, −174.6
26		*c*-Hex	24	**26b**	80	Oil	2.9
27		*i*-Pr	20	**27b**	90	Oil	31.5
28		Ph	12	**28b**	85	71–72	−243.1
29	OAc	Me	48	**29a**	76	206–210	−171.4, −184.6
30		Et	24	**30b**	90	41–43	−171.0
31		*n*-Bu	48	**31a/31b** (52:48)			−205.9, −220.6/−156.3
32		*n*-Oct	48	**32b**	80		−206.6, −221.3/−151.1
33		*c*-Hex	24	**33b** [j]	91	50–54	−215.3
34		*i*-Pr	20	**34b**	89	38–42	−205.9
35		Ph	24	**35b**	92	120–130	−116.1

[a] Poor yield (see text).
[b] The ^{119}Sn-NMR shows ten signals between the range of −82.0 and −140.7 ppm.
[c] Twelve signals between the range of −140.0 and −190.0 ppm.
[d] Seventeen signals between the range of −15.0 and −25.5 ppm.
[e] Poor yield (see text).
[f] Twelve signals between the range of −131.5 and −153.5 ppm.
[g] An additional signal at 89.8 ppm.
[h] An additional signal at 92.4 ppm.
[i] Seven signals between the range of −31.9 and −176.5 ppm.
[j] Isolated as water adduct [45].

(total reaction time 48 h), the ^{119}Sn-NMR spectrum ($CDCl_3$) of which revealed eight signals between −80 and −181 ppm. The signals were unambiguously assigned to [*n*-Bu_2(OH)SnOSn(Br)*n*-Bu_2]$_2$ (**17d**, δ (^{119}Sn): −161.0, −174.5; total integral 22%) [42], [*n*-Bu_2(OH)SnOSn(Br)*n*-Bu_2][*n*-Bu_2(Br)SnOSn(Br)*n*-Bu_2] (**17c**, δ (^{119}Sn): −79.8, −120.9, −154.6, −181.4; total integral 35%), and [*n*-Bu_2(Br)SnOSn(Br)*n*-Bu_2]$_2$ (**17a**, δ (^{119}Sn): −81.3, −129.8; total integral 43%) [42]. These results also suggest that the reaction mechanism appears to involve the initial formation of tetrahydroxide species [*n*-Bu_2(OH)SnOSn(OH)*n*-Bu_2]$_2$ from which hydroxides are replaced in a stepwise fashion by bromides.

2.1.4. Reactions of $(R_2SnO)_n$ with NH_4I

The reaction of $(R_2SnO)_n$ with NH_4I afforded only dimeric tetraorganodistannoxanes 'a' for R = *n*-Bu (**24a**) and *n*-Oct (**25a**), whereas diorganotin diiodides 'b' were isolated for R = Me (**22b**), *c*-Hex (**26b**), *i*-Pr (**27b**) and Ph (**28b**). In the case of R = Et, only a complex mixture was obtained, which could not be

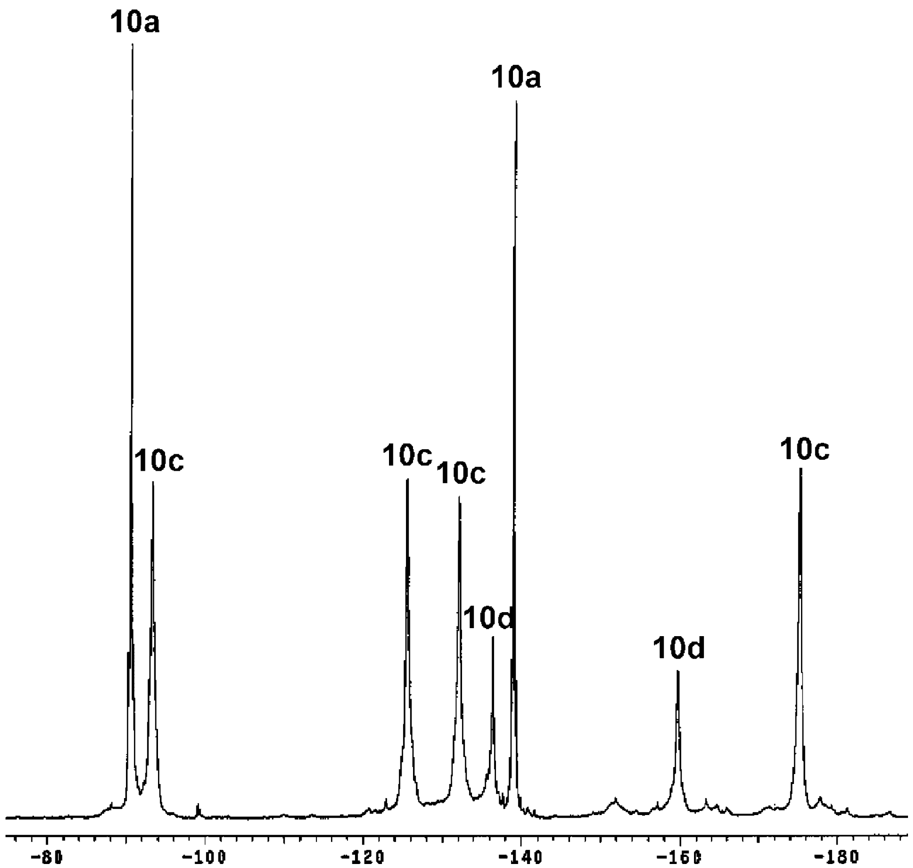

Fig. 1. ^{119}Sn-NMR spectrum ($CDCl_3$) from the reaction of $(n\text{-}Bu_2SnO)_n$ with NH_4Cl after 12 h. Signals denoted with '**10a**', '**10c**' and '**10d**' were assigned to $[n\text{-}Bu_2(Cl)SnOSn(Cl)n\text{-}Bu_2]_2$, $[n\text{-}Bu_2(OH)SnOSn(Cl)n\text{-}Bu_2][n\text{-}Bu_2(Cl)SnOSn(Cl)n\text{-}Bu_2]$ and $[n\text{-}Bu_2(OH)SnOSn(Cl)n\text{-}Bu_2]_2$, respectively.

separated. The ^{119}Sn-NMR spectrum of this mixture revealed seven signals between −30 and −200 ppm.

2.1.5. Reactions of $(R_2SnO)_n$ with NH_4OAc

The reaction of $(R_2SnO)_n$ with NH_4OAc afforded only one dimeric tetraorganodistannoxane, namely, $[Me_2(AcO)SnOSn(OAc)Me_2]_2$ (**29a**), and on almost all other occasions, diorganotin diacetates, $R_2Sn(OAc)_2$ (R = Et (**30b**), *n*-Oct (**32b**), *c*-Hex (**33b**), *i*-Pr (**34b**) and Ph (**35b**)). For $(n\text{-}Bu_2SnO)_n$, a mixture of $[n\text{-}Bu_2(AcO)SnOSn(OAc)n\text{-}Bu_2]_2$ (**31a**; δ (^{119}Sn): −205.9, −220.6; total integral 52%) [42] and $n\text{-}Bu_2Sn(OAc)_2$ (**31b**; δ (^{119}Sn): −156.3; total integral 48%) was obtained. It is worth mentioning that $c\text{-}Hex_2Sn(OAc)_2$ (**33b**) was isolated as its water adduct $c\text{-}Hex_2Sn(OAc)_2\cdot H_2O$, the molecular structure of which has been published elsewhere [45]. The coordination number of tin in $c\text{-}Hex_2Sn(OAc)_2\cdot H_2O$ is seven, which is also reflected in the ^{119}Sn-MAS-NMR resonance being observed at −401.8 ppm. The ^{119}Sn-NMR spectrum of the $c\text{-}Hex_2Sn(OAc)_2\cdot H_2O$ in $CDCl_3$ shows a signal at −215.3 ppm, consistent with pentacoordinate tin atoms and, indicating dissociation of the water.

2.1.6. Synthesis of $[c\text{-}Hex_2(F)SnOSn(Cl)c\text{-}Hex_2]_2$ (36)

Recently, redistribution reactions were described between two symmetric dimeric tetraorganodistannoxanes, $[R_2(X)SnOSn(X)R_2]_2$ and $[R_2(Y)SnOSn(Y)R_2]_2$ [43,37,46,47]. In the example where X and Y represent a combination of a strong and a weak donor, e.g. X = F, Y = Cl or X = OH, Y = Cl, these reactions quantitatively provide unsymmetric dimeric tetraorganodistannoxanes, $[R_2(X)SnOSn(Y)R_2]_2$, whereas equilibria were observed when X and Y both comprise weak donors, e.g. X = Cl, Y = Br. In order to prepare a rare example [37] of dimeric tetraorganodistannoxane containing F and Cl atoms, $[c\text{-}Hex_2(F)SnOSn(F)c\text{-}Hex_2]_2$ (**5a**) and $[c\text{-}Hex_2(Cl)SnOSn(Cl)c\text{-}Hex_2]_2$ (**12a**) were reacted providing $[c\text{-}Hex_2(F)SnOSn(Cl)c\text{-}Hex_2]_2$ (**36**) in almost quantitative yields (Eq. (2)).

$$\mathbf{5a} + \mathbf{12a} \xrightarrow[100\ ^{\circ}\mathrm{C}]{\text{toluene}} \underset{\mathbf{36}}{[c\text{-}Hex_2(F)SnOSn(Cl)c\text{-}Hex_2]_2} \qquad (2)$$

Compound (**36**) is colourless, high-melting solid, which is poorly soluble in common organic solvents. However, it was possible to obtain a ^{119}Sn-NMR spectrum (d_8-toluene) at 100 °C that displays a doublet and a doublet of doublets centred at −175.3 ppm ($^{1}J(^{119}\text{Sn}-^{19}\text{F}) = 1240$ Hz; $^{2}J(^{119}\text{Sn}-\text{O}-^{117/119}\text{Sn}) = 220$ Hz) and −226.1 ppm ($^{1}J(^{119}\text{Sn}-^{19}\text{F}) = 1540$ Hz; $^{2}J(^{119}\text{Sn}-\text{O}-^{117/119}\text{Sn}) = 221/217$ Hz; $^{3}J(^{119}\text{Sn}-\text{OSn}-^{19}\text{F}) = 32$ Hz) of equal intensity (total integral 80%). Additionally, the spectrum shows 15 low intensity signals between −135 and −247 ppm (total integral 20%), which, appear to be systematically related to **36** [48]. No definitive assignment of these signals could be made. The ^{19}F-NMR spectrum of **36** (d_8-toluene, r.t.) reveals one major signal at −124.1 ppm ($^{1}J(^{19}\text{F}-^{117/119}\text{Sn}) = 1220$ Hz; $^{1}J(^{19}\text{F}-^{117/119}\text{Sn}) = 1489$ Hz) and two minor signals at −123.2 and 123.5 ppm, respectively. The ^{119}Sn-MAS-NMR spectrum of **36** shows three signals at −183.0 ($^{1}J(^{119}\text{Sn}-^{19}\text{F}) = 1150$ Hz), −226.0 ($^{1}J(^{119}\text{Sn}-^{19}\text{F}) = 1550$ Hz) and −234.0 ppm ($^{1}J(^{119}\text{Sn}-^{19}\text{F}) = 1630$ Hz) with a total manifold integration of 2:1:1. The number of signals is consistent with the existence of a non-symmetric tetrameric unit or two independent molecules in the crystallographic unit cell, each situated about a centre. The crystallographic study provides evidence for this (see below).

2.2. *Molecular structures of dimeric tetraorganodistannoxanes **29a**, **20a**, **5a**, **36***

The molecular structures of **29a**, **20a**, **5a** and **36** are shown in Figs. 2–5, respectively, and selected bond lengths and angles are listed in Tables 2 and 3. The molecular structure of **29a** represents a second polymorph of the compound with the monoclinic polymorph also crystallising in a non-centrosymmetric space group *Pa* (see Section 3) [49]. Of the structures with the general formula $\{[\text{R}_2\text{Sn}(\text{O}_2\text{CR}')]_2\text{O}\}_2$ (**29a**), i.e. with R = R′ = Me, is an atypical structure, being the sole example of one of five motifs known for compounds of this type [50,51]. The structure is constructed about a central $(\text{Me}_2\text{Sn})_2\text{O}_2$ core to which is linked, via the oxygen atoms, two Me_2Sn entities. Further links between the *endo*-cyclic Sn(1) and Sn(2) atoms, and *exo*-cyclic Sn(3) and Sn(4) atoms, with the exception of the Sn(1) and Sn(4) pair, are afforded by bidentate bridging acetate groups that form essentially symmetric Sn–O bonds. The coordination geometry about the Sn(4) atom is

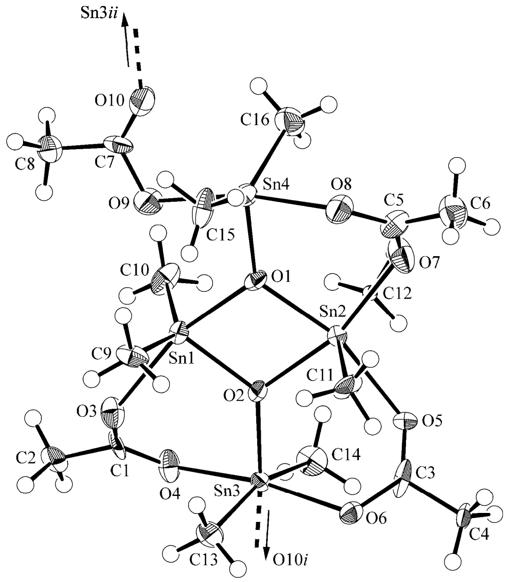

Fig. 2. Molecular structure and crystallographic numbering scheme employed for compound **29a**.

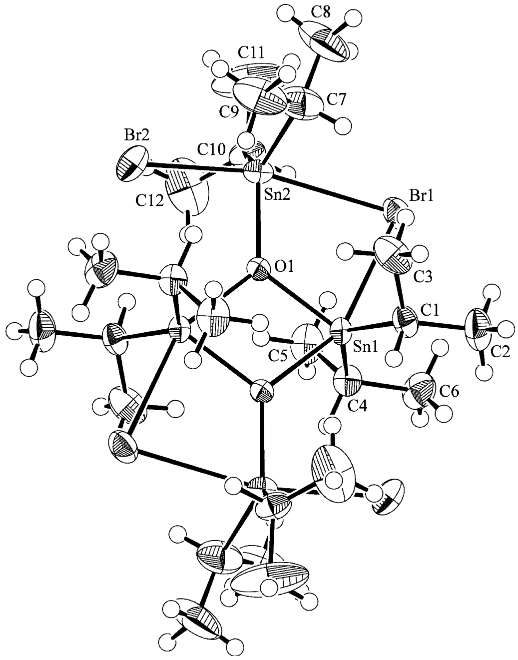

Fig. 3. Molecular structure and crystallographic numbering scheme employed for compound **20a**.

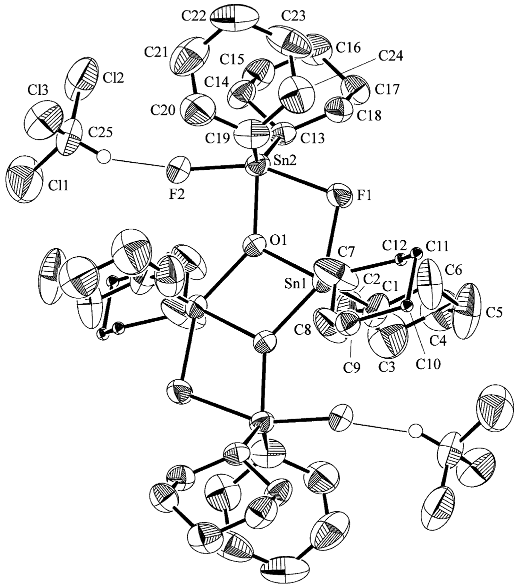

Fig. 4. Molecular structure and crystallographic numbering scheme employed for compound **5a**.

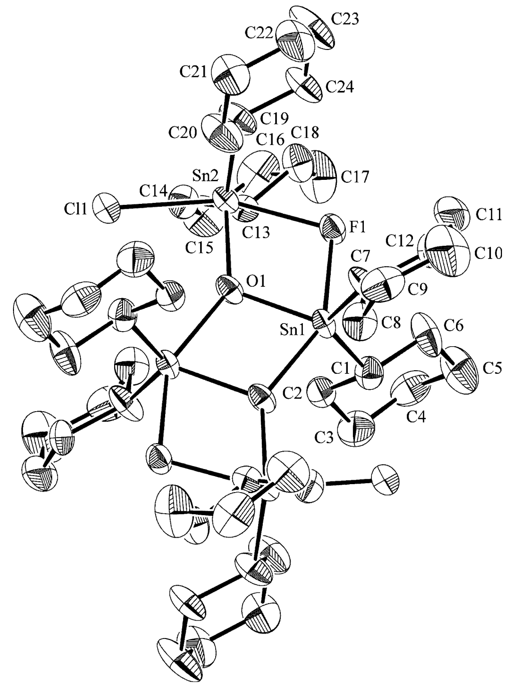

Fig. 5. Molecular structure and crystallographic numbering scheme employed for one of the two independent molecules of compound **36**.

completed by a monodentate acetate ligand. Bridges between neighbouring tetrameric units are present so that the O(10) atom forms an interaction with a symmetry related Sn(3) atom (symmetry operation: $1-x$, $1-y$, $1/2+z$). The Sn(3)–O(10) distance of 2.523(12) Å is not so much longer than the other Sn–$O_{acetate}$ bond distances, which lie in the range 2.212(9)–2.329(13) Å, and hence, the structure is properly described as polymeric with the chain extending along the crystallographic z-axis. The Sn(1) and Sn(4) atom exist in distorted trigonal-bipyramidal geometries with the O(1) and O(3), and O(1) and O(5) atoms defining the axial positions, respectively. A close intramolecular contact between the Sn(1) and O(9) atoms of 2.904(11) Å is not considered to represent a significant bonding interaction between these atoms but may be responsible for the expansion of the C(9)–Sn(1)–C(10) angle to 141.8(5)°. Similarly, a close contact between the Sn(4) and O(10) atoms of 2.881(11) Å is noted which is also probably responsible for the widening of the C(15)–Sn(4)–C(16) angle to 140.8(8)°. By contrast to the trigonal-bipyramidal geometries found for Sn(1) and Sn(4), a skew-trapezoidal-bipyramidal geometry, defined by a C_2O_4 donor set, is the best description for the coordination geometry for the Sn(2) atom where the methyl groups lie over the weaker Sn(2)–O(5), O(7) bonds. A C_2O_4 donor set is also found about the Sn(3) atom which tends towards a distorted octahedral geometry based on a consideration of the angles, the disparity in the Sn–O bond distances notwithstanding.

Table 2
Selected geometric parameters (Å, °) for compound **29a** [a]

Bond lengths			
Sn(1)–O(1)	2.096(11)	Sn(1)–O(2)	2.038(10)
Sn(1)–O(3)	2.303(10)	Sn(1)–C(9)	2.101(12)
Sn(1)–C(10)	2.099(12)	Sn(2)–O(1)	2.073(9)
Sn(2)–O(2)	2.119(10)	Sn(2)–O(5)	2.376(10)
Sn(2)–O(7)	2.329(13)	Sn(2)–C(11)	2.092(11)
Sn(2)–C(12)	2.104(11)	Sn(3)–O(2)	2.049(13)
Sn(3)–O(4)	2.235(9)	Sn(3)–O(6)	2.212(9)
Sn(3)–O(10)^{i}	2.523(12)	Sn(3)–C(13)	2.088(14)
Sn(3)–C(14)	2.097(14)	Sn(4)–O(1)	2.026(12)
Sn(4)–O(8)	2.219(11)	Sn(4)–O(9)	2.229(11)
Sn(4)–C(15)	2.125(14)	Sn(4)–C(16)	2.133(16)
Bond angles			
O(1)–Sn(1)–O(2)	77.1(3)	O(1)–Sn(1)–O(3)	165.1(4)
O(1)–Sn(1)–C(9)	95.6(4)	O(1)–Sn(1)–C(10)	100.3(5)
O(2)–Sn(1)–O(3)	89.0(4)	O(2)–Sn(1)–C(9)	111.8(5)
O(2)–Sn(1)–C(10)	105.6(5)	O(3)–Sn(1)–C(9)	84.3(4)
O(3)–Sn(1)–C(10)	88.7(6)	C(9)–Sn(1)–C(10)	141.8(5)
O(1)–Sn(2)–O(2)	75.9(3)	O(1)–Sn(2)–O(5)	162.5(4)
O(1)–Sn(2)–O(7)	88.2(5)	O(1)–Sn(2)–C(11)	99.6(5)
O(1)–Sn(2)–C(12)	102.2(5)	O(2)–Sn(2)–O(5)	86.6(4)
O(2)–Sn(2)–O(7)	164.0(5)	O(2)–Sn(2)–C(11)	97.2(6)
O(2)–Sn(2)–C(12)	99.5(5)	O(5)–Sn(2)–O(7)	109.3(3)
O(5)–Sn(2)–C(11)	82.4(6)	O(5)–Sn(2)–C(12)	80.4(6)
O(7)–Sn(2)–C(11)	86.7(7)	O(7)–Sn(2)–C(12)	82.3(6)
C(11)–Sn(2)–C(12)	155.1(5)	O(2)–Sn(3)–O(4)	93.8(4)
O(2)–Sn(3)–O(6)	95.6(4)	O(2)–Sn(3)–O(10)^{i}	174.6(3)
O(2)–Sn(3)–C(13)	99.6(5)	O(2)–Sn(3)–C(14)	100.5(5)
O(4)–Sn(3)–O(6)	170.6(5)	O(4)–Sn(3)–O(10)^{i}	80.9(4)
O(4)–Sn(3)–C(13)	91.4(5)	O(4)–Sn(3)–C(14)	87.0(5)
O(6)–Sn(3)–O(10)^{i}	89.8(4)	O(6)–Sn(3)–C(13)	86.9(5)
O(6)–Sn(3)–C(14)	91.4(5)	O(10)^{i}–Sn(3)–C(13)	80.1(5)
O(10)^{i}–Sn(3)–C(14)	79.9(5)	C(13)–Sn(3)–C(14)	159.9(7)
O(1)–Sn(4)–O(8)	92.1(4)	O(1)–Sn(4)–O(9)	79.6(4)
O(1)–Sn(4)–C(15)	112.0(6)	O(1)–Sn(4)–C(16)	106.9(6)
O(8)–Sn(4)–O(9)	168.7(4)	O(8)–Sn(4)–C(15)	84.3(6)
O(8)–Sn(4)–C(16)	90.1(6)	O(9)–Sn(4)–C(15)	91.6(5)
O(9)–Sn(4)–C(16)	99.7(6)	C(15)–Sn(4)–C(16)	140.8(8)
Sn(1)–O(1)–Sn(2)	103.2(5)	Sn(1)–O(1)–Sn(4)	125.0(4)
Sn(2)–O(1)–Sn(4)	131.8(5)	Sn(1)–O(2)–Sn(2)	103.6(6)
Sn(1)–O(2)–Sn(3)	128.8(5)	Sn(2)–O(2)–Sn(3)	127.6(4)
Sn(1)–O(3)–C(1)	130.6(8)	Sn(3)–O(4)–C(1)	127.0(9)
Sn(2)–O(5)–C(3)	127.8(9)	Sn(3)–O(6)–C(3)	123.4(10)
Sn(2)–O(7)–C(5)	130.8(11)	Sn(4)–O(8)–C(5)	128.6(11)
Sn(4)–O(9)–C(7)	108.1(9)	Sn(3)–O(10)^{i}–C(7)^{i}	149.7(10)

[a] Symmetry operation i, $1-x$; $1-y$; $1/2+z$.

As mentioned above, **29a** is one of two polymorphs for which full structure determinations are available.

In our hands, **29a** crystallised as a mixture of different polymorphs from a solution of $CHCl_3$–hexane (1:2) within 3 days, as evidenced by the number of ^{119}Sn-MAS-NMR signals (ca. 6). The exact number of signals could not be determined owing to problems with overlapping spinning sidebands. From this mixture, a crystal was selected for the X-ray structure analysis, which showed a new polymorph for **29a**. The molecular structures for the two polymorphs are in essential agreement with each other. The lack of crystallographic

Table 3
Selected geometric parameters (Å, °) for compounds **20a**, **5a** and **36**

	20a [a]	**5a** [b]	**36** (molecule a) [c]		**36** (molecule b)
Bond lengths					
Sn(1)–O(1)	2.058(3)	2.042(4)	2.071(4)	Sn(3)–O(2)	2.060(4)
Sn(1)–O(1)^{i}	2.161(3)	2.115(4)	2.113(4)	Sn(3)–O(2)^{i}	2.132(4)
Sn(1)–X(1)	2.8222(9)	2.174(4)	2.157(3)	Sn(3)–F(2)	2.170(4)
Sn(1)–C(1)	2.167(5)	2.128(9)	2.146(7)	Sn(3)–C(25)	2.147(6)
Sn(1)–C(a)	2.153(6)	2.124(9)	2.146(6)	Sn(3)–C(31)	2.156(6)
Sn(2)–O(1)	2.034(3)	2.011(4)	2.023(4)	Sn(4)–O(2)	2.021(4)
Sn(2)–X(1)	2.9542(17)	2.241(4)	2.277(4)	Sn(4)–F(2)	2.231(4)
Sn(2)–Y	2.5995(16)	2.011(4)	2.4541(16)	Sn(4)–Cl(2)	2.4443(18)
Sn(2)–C(b)	2.164(7)	2.138(6)	2.143(6)	Sn(4)–C(37)	2.147(5)
Sn(2)–C(c)	2.164(6)	2.142(7)	2.171(7)	Sn(4)–C(43)	2.138(8)
Bond angles					
O(1)–Sn(1)–O(1)^{i}	74.82(14)	73.93(18)	74.76(18)	O(2)–Sn(3)–O(2)^{i}	73.76(18)
O(1)–Sn(1)–X(1)	80.24(9)	72.68(15)	73.07(14)	O(2)–Sn(3)–F(2)	72.94(14)
O(1)–Sn(1)–C(1)	112.72(19)	115.6(3)	116.3(2)	O(2)–Sn(3)–C(25)	112.59(19)
O(1)–Sn(1)–C(a)	111.05(18)	115.2(4)	111.7(3)	O(2)–Sn(3)–C(31)	109.9(2)
O(1)^{i}–Sn(1)–X(1)	155.06(9)	146.51(15)	147.82(15)	O(2)^{i}–Sn(3)–F(2)	146.70(15)
O(1)^{i}–Sn(1)–C(1)	99.28(18)	98.3(3)	99.8(2)	O(2)^{i}–Sn(3)–C(25)	99.7(2)
O(1)^{i}–Sn(1)–C(a)	98.57(18)	101.4(3)	103.3(2)	O(2)^{i}–Sn(3)–C(31)	102.73(18)
X(1)–Sn(1)–C(1)	89.95(15)	98.2(3)	93.5(2)	F(2)–Sn(3)–C(25)	92.8(2)
X(1)–Sn(1)–C(a)	90.56(16)	90.4(3)	89.5(2)	F(2)–Sn(3)–C(31)	88.74(19)
C(1)–Sn(1)–C(a)	135.6(2)	128.7(4)	130.5(3)	C(25)–Sn(3)–C(31)	136.0(2)
O(1)–Sn(2)–X(1)	77.35(10)	71.81(15)	71.40(15)	O(2)–Sn(4)–F(2)	72.35(14)
O(1)–Sn(2)–Y	89.44(10)	84.73(16)	87.12(12)	O(2)–Sn(4)–Cl(2)	90.80(12)
O(1)–Sn(2)–C(b)	113.7(2)	113.3(2)	109.1(2)	O(2)–Sn(4)–C(37)	111.1(2)
O(1)–Sn(2)–C(c)	116.48(18)	109.7(3)	115.7(2)	O(2)–Sn(4)–C(43)	114.5(3)
X(1)–Sn(2)–Y	166.77(2)	156.52(14)	158.49(9)	F(2)–Sn(4)–Cl(2)	163.02(10)
X(1)–Sn(2)–C(b)	86.7(2)	92.9(2)	84.84(19)	F(2)–Sn(4)–C(37)	86.71(19)
X(1)–Sn(2)–C(c)	87.15(17)	89.0(3)	91.5(2)	F(2)–Sn(4)–C(43)	87.7(4)
Y–Sn(2)–C(b)	99.6(2)	97.5(2)	103.90(17)	Cl(2)–Sn(4)–C(37)	101.79(17)
Y–Sn(2)–C(c)	98.18(18)	98.1(3)	96.9(2)	Cl(2)–Sn(4)–C(43)	97.7(3)
C(b)–Sn(2)–C(c)	126.5(3)	135.2(3)	131.2(2)	C(37)–Sn(4)–C(43)	129.7(3)
Sn(1)–O(1)–Sn(2)	124.71(16)	113.9(2)	114.05(18)	Sn(3)–O(2)–Sn(4)	113.18(17)
Sn(1)^{i}–O(1)–Sn(2)	130.10(17)	138.6(2)	140.7(2)	Sn(3)–O(2)–Sn(4)^{i}	140.5(2)
Sn(1)–O(1)–Sn(1)^{i}	105.18(14)	106.07(18)	105.24(18)	Sn(3)–O(2)–Sn(3)^{i}	106.24(18)
Sn(1)–X(1)–Sn(2)	77.69(3)	100.64(14)	101.48(14)	Sn(3)–F(2)–Sn(4)	101.42(13)

Symmetry operation i: $-x, -y, -z$; $1/2-x, 1/2-y, 1-z$; $-x, 1-y, -z$; $-x, -y, -1-z$.

[a] X = Br; Y = Br(2); $a = 4$; $b = 7$; $c = 10$.

[b] X = F; Y = F(2); $a = 7$; $b = 13$; $c = 19$.

[c] X = F; Y = Cl(1); $a = 7$; $b = 13$; $c = 19$.

symmetry in **29a** is unusual and indeed the remaining structures of **20a**, **5a** and **36** are centrosymmetric.

The molecular structure of **20a** shows a centrosymmetric $(i\text{-}Pr_2Sn)_2O_2$ core connected, via the oxygen atoms, to two i-Pr_2Sn entities. Almost symmetric bromide bridges between the *endo*- and *exo*-cyclic tin atoms are present. The Sn(2)–bound Br(2) atoms are terminal in that the intramolecular Sn(1)···Br(2) separations of 3.530(3) Å are not indicative of significant bonding interactions between these atoms. The coordination geometries for the tin atoms are both based on trigonal-bipyramids. In the case of Sn(1), the O(1) and Br(1) atoms occupy the axial positions, and two bromides occupy the axial positions about the Sn(2) atom. The influence of the close Sn(1)···Br(2) interaction is such to expand the C(1)–Sn(1)–C(4) angle to 135.6(2)° compared with 126.5(3)° for C(7)–Sn(2)–C(10). The ^{119}Sn-MAS-NMR spectrum of **20a** showing two signals at −72.0 and −148.0 ppm, is in agreement with the centrosymmetric space group found in the X-ray diffraction experiment. The molecular structure of the fluoride analogue, **5a**, is in essential agreement with that of **20a**.

Allowing for the replacement of the bromides by fluorides and the substitution of the isopropyl substituents with cyclohexyl, the structure of **5a** is as described above for **20a**. The intramolecular Sn(1)···F(2) separations are 3.472(4) Å. The key difference between the two structures is found in the association of two chloroform molecules to the tetrameric unit as illustrated in Fig. 4. Hydrogen bonding interactions between the terminal F(2) atoms are noted so that H···F(2) is 1.91 Å, C(25)···F(2) is 2.868(10) Å and the angle subtended at H is 161°. While full details are not reported here, a preliminary structure of the chloride analogue, **12a**, has been determined. Difficulties in the refinement owing to the lack of resolution of two cyclohexyl rings preclude a full report but suffice to say that the structure resembles very closely the prototype **5a**. The final structure determined is an example of a novel mixed halide, i.e. **36**.

The structure of **36** crystallises with two independent centrosymmetric molecules comprising the asymmetric unit. One of the molecules is shown in Fig. 5 and the other is in essential agreement with this. Selected geometric parameters for both independent molecules are collected in Table 3. From Fig. 5, it is apparent that the more electronegative fluorine atoms function as symmetric bridges between the *endo*- and *exo*-cyclic tin atoms. The chlorine atoms occupy terminal positions with Sn(1)···Cl(1) being 3.707(3) Å and Sn(3)···Cl(2) being 3.814(3) Å, distances again not indicative of significant bonding interactions. Very recently, the crystal structure of the phenyl analogue was reported, i.e. $[Ph_2(F)SnOSn(Cl)Ph_2]_2$ [52]. In this structure, the fluoride bridges are similar with Sn(1)–F(1) and Sn(2)–F(1) being 2.175(4) and 2.222(5) Å, respectively and the Sn(1)···Cl(1) separation is 3.663(2) Å [52].

3. Experimental

3.1. General methods

The diorganotin oxides $(n\text{-}Bu_2SnO)_n$ and $(n\text{-}Oct_2SnO)_n$ were commercially available (Aldrich, Ventron), whereas $(Me_2SnO)_n$, $(Et_2SnO)_n$, $(i\text{-}Pr_2SnO)_n$, $(c\text{-}Hex_2SnO)_n$ and $(Ph_2SnO)_n$ were prepared according to literature procedures [41]. ^{119}Sn-NMR (100.74 MHz) and ^{19}F-NMR (254.19 MHz) spectra were recorded using a JEOL-GX 270 MHz FT-NMR spectrometer and are referenced to Me_4Sn and $CFCl_3$, respectively. ^{1}H-NMR (299.98 MHz) and ^{13}C-NMR (75.44 MHz) were obtained on a Varian 300 MHz Unity Plus NMR spectrometer, and are referenced to Me_4Si. All chemical shifts were recorded in $CDCl_3$, unless otherwise indicated. ^{119}Sn-MAS-NMR spectra were recorded using a JEOL Eclipse Plus 400 MHz FT-NMR spectrometer, referenced to Me_4Sn. Uncorrected melting points (m.p.) were determined on a Reichert hot stage. Microanalyses were performed at the Australia National University (Canberra, Australia) or by CMAS Belmont (Geelong, Australia).

3.2. General procedure for the reaction of $(R_2SnO)_n$ with NH_4X

The organotin oxide, $(R_2SnO)_n$, (10.0 mmol, 1.65 g for R = Me, 1.93 g for R = Et, 2.49 g for R = *n*-Bu, 3.61 g for R = *n*-Oct, 3.01 g for R = *c*-Hex, 2.21 g for R = *i*-Pr, 2.89 g for R = Ph) was suspended in 1,4-dioxane (50 ml) and a saturated aqueous solution (50 ml) of the appropriate NH_4X (X = F, Cl, Br, I, OAc) was added. The reaction mixture was heated under reflux until all of the $(R_2SnO)_n$ had dissolved (cf. Table 1). Then, the solvent mixture was almost entirely removed in vacuo and the resulting residue was extracted with $CHCl_3$ (2 × 100 ml). The combined organic extracts were dried over Na_2SO_4. After removal of the solvent, a crude product was obtained, which was recrystallised from chloroform–hexane.

For $(Me_2SnO)_n$–NH_4F a complex mixture was obtained (0.33 g). No pure product could be isolated (see text).

For $(Et_2SnO)_n$–NH_4F a complex mixture was obtained (0.49 g). No pure product could be isolated (see text).

3.2.1. $[n\text{-}Bu_2(F)SnOSn(F)n\text{-}Bu_2]_2$ (**3a**)

White solid (1.95 g, 75%, m.p. 180–185 °C (Lit. m.p. 115–117 °C) [4]). ^{1}H-NMR: $\delta = 0.91$–0.97 (m, 24H), 1.35–1.51 (m, 32H), 1.63–1.73 (m, 16H). ^{13}C-NMR: $\delta = 13.5$, 23.1 ($^{1}J(^{13}C-^{117/19}Sn) = 591/618$ Hz), 24.0 ($^{1}J(^{13}C-^{117/19}Sn) = 567/594$ Hz), 26.7, 26.8. ^{19}F-NMR: $\delta = -132.4$ ($^{1}J(^{19}F-^{117/119}Sn) = 741$ Hz, $^{1}J(^{19}F-^{117/119}Sn) = 1763$ Hz). ^{119}Sn-NMR: $\delta = -142.2$ (t, $^{1}J(^{119}Sn-^{19}F) = 771$ Hz), -159.4 (t, $^{1}J(^{119}Sn-^{19}F) = 1795$ Hz). Anal. Calc. for $C_{32}H_{72}F_4O_2Sn_4$ (1039.7): C, 37.0; H, 7.0. Found: C, 37.4; H, 7.6%.

For $(n\text{-}Oct_2SnO)_n$–NH_4F a complex mixture was obtained (2.50 g). No pure product could be isolated (see text).

3.2.2. $[c\text{-}Hex_2(F)SnOSn(F)c\text{-}Hex_2]_2$ (**5a**)

Colourless solid (2.68 g, 86%, m.p. (dec.) > 295 °C). ^{1}H-NMR: $\delta = 1.20$–2.50 (m). ^{13}C-NMR: $\delta = 26.8$, 28.8, 28.9, 30.2, 30.4, 42.0, 42.2. ^{19}F-NMR: $\delta = -144.9$ ($^{1}J(^{19}F-^{117/119}Sn_{endo}) = 723$, $^{1}J(^{19}F-^{117/119}Sn_{endo}) = 822$ Hz, $^{1}J(^{19}F-^{117/119}Sn_{exo}) = 1875/1956$ Hz). ^{119}Sn-NMR: $\delta = -237.6$ (t, $^{1}J(^{119}Sn-^{19}F) = 1950$ Hz), -212.0 (t, $^{1}J(^{119}Sn-^{19}F)$ 778 Hz). Anal. Calc. for $C_{48}H_{88}F_4O_2Sn_4$ (1248.0): C, 46.2; H, 7.1. Found: C, 46.3; H, 7.2%.

For $(i\text{-}Pr_2SnO)_n$–NH_4F a complex mixture was obtained (1.80 g). No pure product could be isolated (see text). For $(Ph_2SnO)_n$–NH_4F a complex mixture was obtained (0.58 g). No pure product could be isolated (see text).

3.2.3. $[Me_2(Cl)SnOSn(Cl)Me_2]_2$ (**8a**)

White solid (1.58 g, 82%, m p. > 280 °C (Lit. m.p. > 300 °C) [4]). ^{119}Sn-NMR: $\delta = -62.6, -114.4$.

3.2.4. $[Et_2(Cl)SnOSn(Cl)Et_2]_2$ (**9a**)

White solid (1.32 g, 60%, m.p. 168–170 °C (Lit. m.p. 175.5–176.5 °C) [4]). ^{119}Sn-NMR: $\delta = -89.1, -137.6$.

3.2.5. $[n\text{-}Bu_2(Cl)SnOSn(Cl)n\text{-}Bu_2]_2$ (**10a**)

White solid (2.65 g, 96%, m.p. 110–111 °C (Lit. m.p. 112–114 °C) [4]). ^{119}Sn-NMR: $\delta = -91.4$ ($^2J(^{117}\text{Sn–O–}^{119}\text{Sn}) = 74$ Hz), -140.3 ($^2J(^{117}\text{Sn–O–}^{119}\text{Sn}) = 71$ Hz).

3.2.6. $[n\text{-}Oct_2(Cl)SnOSn(Cl)n\text{-}Oct_2]_2$ (**11a**)

White solid (3.58 g, 92%, m.p. 95 °C). ^{1}H-NMR: $\delta =$ 0.88 (broad s, 12H), 1.29 (broad s, 34H), 1.78 (broad s, 4H), 1.81 (broad s, 18H). ^{13}C-NMR: $\delta = 14.0$, 14.0, 22.6, 22.6, 25.0, 25.2, 29.1, 29.2, 29.2, 31.8, 31.9, 33.1, 33.2, 33.5, 33.6. ^{119}Sn-NMR: $\delta = -90.8$ ($^2J(^{117}\text{Sn–O–}^{119}\text{Sn}) = 69$ Hz), -138.2 ($^2J(^{117}\text{Sn–O–}^{119}\text{Sn}) = 71$ Hz). ^{119}Sn-MAS-NMR: $\delta = -84.0, -141.0$. Anal. Calc. for $C_{64}H_{136}Cl_4O_2Sn_4$ (1554.4): C, 49.5; H, 8.8. Found: C, 48.5; H, 9.0%.

3.2.7. $[c\text{-}Hex_2(Cl)SnOSn(Cl)c\text{-}Hex_2]_2$ (**12a**)

Colourless solid (2.76 g, 84%). M p.(dec.) > 250 °C. ^{1}H-NMR: $\delta = 1.20–2.50$ (m). ^{13}C-NMR: $\delta = 26.2$, 26.7, 26.8, 28.3, 29.0, 29.9, 30.5, 31.3. ^{119}Sn-NMR: $\delta = -139.0$, -202.7 ($^2J(^{117}\text{Sn–O–}^{119}\text{Sn}) = 89$ Hz). Anal. Calc. for $C_{48}H_{88}Cl_4O_2Sn_4$ (1313.9): C, 43.9; H, 6.8. Found: C, 43.0; H, 6.5%.

3.2.8. $[Et_2(Br)SnOSn(Br)Et_2]_2$ (**16a**)

White solid (1.59 g, 60%, m.p. 178 °C (Lit. m.p. 172–173 °C) [3]). ^{1}H-NMR: $\delta = 1.41–1.52$ (m, 24H), 1.86–1.97 (t, 16H). ^{13}C-NMR: $\delta = 9.55$, 10.4, 27.8 ($^1J(^{13}\text{C–}^{117/119}\text{Sn}) = 535/561$ Hz), 29.4 ($^1J(^{13}\text{C–}^{117/119}\text{Sn}) = 586/612$ Hz). ^{119}Sn-NMR: $\delta = -79.3$ ($^2J(^{117}\text{Sn–O–}^{119}\text{Sn}) = 79$ Hz), -128.9 ($^2J(^{117}\text{Sn–O–}^{119}\text{Sn}) = 79$ Hz). Anal. Calc. for $C_{16}H_{40}Br_4O_2Sn_4$ (1058.9): C, 18.2; H, 3.8. Found: C, 18.5; H, 3.7%.

3.2.9. $[n\text{-}Bu_2(Br)SnOSn(Br)n\text{-}Bu_2]_2$ (**17a**)

White solid (3.05 g, 95%, m.p. 104 °C (Lit. m.p. 107–108 °C) [3]). ^{1}H-NMR: $\delta = 0.93–0.99$ (m, 24H), 1.36–1.57 (m, 16H), 1.70–2.10 (m, 32H). ^{13}C-NMR: $\delta = 13.5$, 13.5, 26.2, 26.4, 27.1 ($^3J(^{13}\text{C–}^{117/119}\text{Sn}) = 33$ Hz), 27.7 ($^3J(^{13}\text{C–}^{117/119}\text{Sn}) = 30$ Hz), 36.0 ($^1J(^{13}\text{C–}^{117/119}\text{Sn}) = 522/547$ Hz), 36.2 ($^1J(^{13}\text{C–}^{117/119}\text{Sn}) = 570/594$ Hz). ^{119}Sn-NMR: $\delta = -81.3$ ($^2J(^{117}\text{Sn–O–}^{119}\text{Sn}) = 79$ Hz), -129.8 ($^2J(^{117}\text{Sn–O–}^{119}\text{Sn}) = 79$ Hz). ^{119}Sn-MAS-NMR: $\delta = -58.4, -136.4$. Anal. Calc. for $C_{32}H_{72}Br_4O_2Sn_4$ (1283.4): C, 30.0; H, 5.7. Found: C, 30.5; H, 5.9%.

3.2.10. $[n\text{-}Oct_2(Br)SnOSn(Br)n\text{-}Oct_2]_2$ (**18a**)

Colourless solid (3.90 g, 90%, m.p. 64 °C). ^{1}H-NMR: $\delta = 0.87$ (broad s, 12H), 1.29 (broad s, 34H), 1.86 (broad s, 4H), 1.90 (broad s, 18H). ^{13}C-NMR: $\delta = 14.1$, 14.1, 22.6, 22.7, 25.1, 25.6, 29.1, 29.2, 29.3, 31.8, 31.9, 33.3, 33.5, 36.4, 33.5. ^{119}Sn-NMR: $\delta = -82.0$ ($^2J(^{117}\text{Sn–O–}^{119}\text{Sn}) = 79$ Hz), -130.1 ($^2J(^{117}\text{Sn–O–}^{119}\text{Sn}) = 79$ Hz). ^{119}Sn-MAS-NMR: $\delta = -74.0, -134.0$. Anal. Calc. for $C_{64}H_{136}Br_4O_2Sn_4$ (1732.2): C, 44.4; H, 7.9. Found: C, 44.3; H, 8.1%.

3.2.11. $[i\text{-}Pr_2(Br)SnOSn(Br)i\text{-}Pr_2]_2$ (**20a**)

Colourless solid (2.34 g, 80%, m.p. (dec.) > 270 °C). ^{1}H-NMR: $\delta = 1.24–1.73$ (m, 48H), 2.20–2.54 (m, 8H). ^{13}C-NMR: $\delta = 20.1$, 21.5 ($^2J(^{13}\text{C–}^{117/19}\text{Sn}) = 18$ Hz), 40.5. ^{119}Sn-NMR: $\delta = -91.9$ ($^2J(^{117}\text{Sn–O–}^{119}\text{Sn}) = 98$ Hz), -144.0 ($^2J(^{117}\text{Sn–O–}^{119}\text{Sn}) = 98$ Hz). ^{119}Sn-MAS-NMR: $\delta = -72.0, -148.0$. Anal. Calc. for $C_{24}H_{56}Br_4O_2Sn_4$ (1171.1): C, 24.6; H; 4.8. Found: C, 24.7; H, 4.8%.

3.2.12. $[Me_2(AcO)SnOSn(OAc)Me_2]_2$ (**29a**)

Colourless solid (1.64 g, 76%, m.p. 206–210 °C (Lit. m.p. 115–117 °C) [49]). ^{1}H-NMR: $\delta = 0.64–0.92$ (m, 24H), 1.95 (s, 12H). ^{13}C-NMR: $\delta = 5.92$ ($^1J(^{13}\text{C–}^{117/119}\text{Sn}) = 715/750$ Hz), 8.72 ($^1J(^{13}\text{C–}^{117/119}\text{Sn}) = 766/800$ Hz), 22.9 (Me), 177.5 (C=O). ^{119}Sn-NMR: $\delta = -171.4$ ($^2J(^{117}\text{Sn–O–}^{119}\text{Sn}) = 103$ Hz), -184.6 ($^2J(^{117}\text{Sn–O–}^{119}\text{Sn}) = 101$ Hz). Anal. Calc. for $C_{16}H_{36}O_{10}Sn_4$ (863.2): C, 22.3; H, 4.2. Found: C, 22.6; H, 4.1%.

3.2.13. $n\text{-}Oct_2Sn(OAc)_2$ (**32b**)

Colourless oil (3.71 g, 80%). ^{1}H-NMR: $\delta = 0.88$ (broad s, 6H), 1.29 (broad s, 28H), 1.67 (broad s, 6H). ^{13}C-NMR: $\delta = 13.9$, 22.5, 24.3, 25.0, 25.5, 29.0, 31.7, 33.1, 181.4 (C=O). ^{119}Sn-NMR: $\delta = -148.1$.

3.2.14. $c\text{-}Hex_2Sn(OAc)_2(H_2O)$ (**33b**)

Colourless solid (1.27 g, 91%, m.p. 50–54 °C). ^{1}H-NMR: $\delta = 0.80–1.99$ (m, 22H), 2.10 (s, 6H). ^{13}C-NMR: $\delta = 20.5$ (Me), 26.3 ($^4J(^{13}\text{C–}^{117/19}\text{Sn}) = 12$ Hz), 28.4 ($^3J(^{13}\text{C–}^{117/119}\text{Sn}) = 100/104$ Hz), 29.6 ($^2J(^{13}\text{C–}^{117/119}\text{Sn}) = 23$ Hz), 42.8 ($^1J(^{13}\text{C–}^{117/19}\text{Sn}) = 517/540$ Hz), 181.4 (C=O). ^{119}Sn-NMR: $\delta = -215.3$. ^{119}Sn-MAS-NMR: $\delta = -401.8$. (discussed in text) IR (KBr) $\nu(H_2O)$: 3394.7 cm^{-1}. Anal. Calc. for $C_{16}H_{30}O_5Sn$ (421.1): C, 45.6; H, 7.2. Found: C, 45.7; H, 7.3%.

3.3. Synthesis of $[c\text{-}Hex_2(F)SnOSn(Cl)c\text{-}Hex_2]_2$ (**36**)

A solution of **5a** (0.11 g, 0.09 mmol) in toluene (2.0 ml) was added to a solution of **12a** (0.12 g, 0.09 mmol) in toluene (2.0 ml) and the mixture was heated at 100 °C for 12 h. The solvent was removed in vacuo and the resulting residue was recrystallised from chloroform–

hexane to afford **36** as colourless crystals (0.111 g, 95%). M.p. (dec.) > 230 °C. ^{1}H-NMR: $\delta = 1.20–2.50$ (m). ^{13}C-NMR: $\delta = 26.8$, 26.9, 28.9, 29.1, 30.7, 30.9, 43.9 ($^{2}J(^{13}C-^{19}F) = 6$ Hz), 44.3 ($^{2}J(^{13}C-^{19}F) = 11$ Hz). ^{19}F-NMR: $\delta = -124.1$ ($^{1}J(^{19}F-^{117/119}Sn) = 1220$ Hz, $^{1}J(^{19}F-^{117/119}Sn) = 1489$ Hz) and minor signals (see text). ^{119}Sn-NMR: $\delta = -175.3$ (d, $^{1}J(^{119}Sn-^{19}F) = 1240$ Hz, $^{2}J(^{119}Sn-O-^{117}Sn) = 220$ Hz), -226.1 (dd, $^{1}J(^{119}Sn-^{19}F) = 1540$ Hz, $^{2}J(^{119}Sn-O-^{117/119}Sn) = 212/217$ Hz, $^{3}J(^{119}Sn-O-Sn-^{19}F) = 32$ Hz) and minor signals (see text). ^{119}Sn-MAS-NMR $\delta = -183.0$ (4Sn, d, $^{1}J(^{119}Sn-^{19}F) = 1150$ Hz), -226.0 (2Sn, d, $^{1}J(^{119}Sn-^{19}F) = 1550$ Hz), -234.0 (2Sn, d, $^{1}J(^{119}Sn-^{19}F) = 1630$ Hz).

Anal. Calc. for $C_{48}H_{88}Cl_2F_2O_2Sn_4$ (1281.0): C, 45.0; H, 6.9. Found: C, 45.9; H, 7.4%.

3.4. Crystallography

Intensity data for colourless crystals of **5a**, **20a** and **29a** were measured at 173 K on a Rigaku AFC7R diffractometer fitted with Mo–K$_{\alpha}$ radiation employing the ω–2θ scan technique in each case. Data for **36** were measured at 223 K on a Bruker AXS SMART CCD diffractometer using Mo–K$_{\alpha}$ radiation and ω-scans. Data were corrected for Lorentz and polarisation effects and for absorption using empirical procedures [53,54]. Crystallographic data and refinement details are summarised in Table 4. The structures were solved using heavy-atom methods [55] and refined by a full-matrix least-squares procedure based on F^2 [56]. All non-H atoms were generally refined with anisotropic displacement parameters (with some exceptions as discussed below) and H atoms were included in the models in their calculated positions in the riding model approximation. The refinements converged after the inclusion of a weighting scheme of the form $w = 1/[\sigma^2(F_o^2) + aP^2 + bP]$ where $P = (F_o^2 + 2F_c^2)/3$. The structure of **29a** was found to crystallise in the non-centrosymmetric space group $Pna2_1$. Final refinement confirmed the choice of space group as the centrosymmetric mate, *Pnma*, would require the molecule to possess a mirror plane or be disposed about a centre of inversion. However, the overall structure is close to centrosymmetric and some difficulties were noted in the refinement. In particular, the C(12) atom was modelled isotropically. Further, a rather large residual electron density peak of 2.46 e Å^{-3} was located in a chemically non-sensible position. The absolute structure was determined on the basis of the value of Flack parameter [57] of 0.15(9). The C(8)–C(12) atoms of a cyclohexyl ring in **5a** were found to be disordered over two positions. The two conformations were assigned equal weight based on the refinement. Similarly, disorder was resolved for the C(46) and C(48) atoms of a cyclohexyl group in **36**. These were assigned site occupancies of 0.55:0.45 from the refinement. The relatively large residual electron density peak in **36** is located 0.86 Å from the Sn(1) atom. Final refinement details are given in Table 4 and the crystallographic numbering schemes are shown in Figs. 2–5

Table 4
Crystallographic data and refinement details for compounds **29a**, **20a**, **5a** and **36**

	29a	**20a**	**5a**	**36**
Formula	$C_{16}H_{36}O_{10}Sn_4$	$C_{24}H_{56}Br_4O_2Sn_4$	$C_{50}H_{90}Cl_6F_4O_2Sn_4$	$C_{48}H_{88}Cl_2F_2O_2Sn_4$
Formula weight	863.2	1171.1	1486.7	1280.8
Crystal system	Orthorhombic	Monoclinic	Monoclinic	Triclinic
Space group	$Pna2_1$	$P2_1/n$	$C2/c$	$P\bar{1}$
a (Å)	16.261(3)	9.396(5)	23.091(4)	11.9959(6)
b (Å)	7.706(4)	18.339(8)	14.263(4)	12.1875(6)
c (Å)	21.583(5)	11.127(9)	20.086(5)	19.4730(9)
α (°)	90	90	90	74.018(1)
β (°)	90	98.72(1)	112.93(1)	88.875(1)
γ (°)	90	90	90	76.026(1)
V (Å^3)	2704(1)	1895(2)	6093(2)	2652.6(2)
Z	4	2	4	2
D_{calc} (cm^{-3})	2.120	2.052	1.621	1.604
μ (cm^{-1})	36.93	68.53	19.30	20.03
F(000)	1648	1112	2976	1288
Crystal size (mm)	0.16 × 0.24 × 0.32	0.11 × 0.16 × 0.32	0.32 × 0.32 × 0.40	0.04 × 0.07 × 0.16
Unique data	3243	4346	7000	15 106
Data with $I \geq 2\sigma(I)$	2831	2747	4468	9534
$R(F^2)$ for observed data	0.034	0.028	0.039	0.055
$wR(F^2)$ for all data	0.114	0.076	0.154	0.146
a	0.0545	0.0111	0.0789	0.0682
b	19.3613	1.3859	33.3785	0
ρ (e Å^{-3})	2.46	0.62	0.92	1.62

which were drawn with ORTEPII [58] at the 50% probability level in each case. Data manipulation was conducted with the TEXSAN suite of programs [59].

4. Supplementary material

Crystallographic data for **29a**, **20a**, **5a** and **36** have been deposited at the Cambridge Crystallographic Data Centre with deposition numbers 185148–185151, respectively. Copies of the information may be obtained free of charge from The Director, CCDC, 12 Union Road, Cambridge CB2 1EZ, UK (Fax: +44-1223-336033; e-mail: deposit@ccdc.cam.ac.uk or www. http://www.ccdc.cam.ac.uk).

Acknowledgements

We wish to thank the Australian Research Council for support of this work.

References

[1] R. Okawara, D.G. White, K. Fujitani, H. Sato, J. Am. Chem. Soc. 83 (1961) 1342.
[2] R. Okawara, Proc. Chem. Soc. (1961) 383.
[3] R. Okawara, M. Wada, J. Organomet. Chem. 1 (1963) 81.
[4] D.L. Alleston, A.G. Davies, M. Hancock, R.F.M. White, J. Chem. Soc. (1963) 5469.
[5] D.L. Alleston, A.G. Davies, M. Hancock, J. Chem. Soc. (1964) 5744.
[6] W.J. Considine, G.A. Baum, R.C. Jones, J. Organomet. Chem. 3 (1965) 308.
[7] K. Yasuda, H. Matsumoto, R. Okawara, J. Organomet. Chem. 6 (1966) 528.
[8] M. Wada, R. Okawara, J. Organomet. Chem. 8 (1967) 261.
[9] Y. Maeda, R. Okawara, J. Organomet. Chem. 10 (1967) 247.
[10] O.R. Floeck, M. Dräger, Organometallics 12 (1993) 4623.
[11] J. Otera, H. Nozak, Tetrahedron Lett. 27 (1986) 5743.
[12] J. Otera, T. Yano, Y. Himeno, H. Nozaki, Tetrahedron Lett. 27 (1986) 4501.
[13] J. Otera, T. Yano, A. Kawabata, H. Nozaki, Tetrahedron Lett. 27 (1986) 2383.
[14] J. Otera, S. Ioka, H. Nozaki, J. Org. Chem. 54 (1989) 4013.
[15] J. Otera, N. Danoh, H. Nozaki, J. Org. Chem. 56 (1991) 5307.
[16] J. Otera, N. Dan-Oh, H. Nozaki, J. Chem. Soc. Chem. Commun. (1991) 1742.
[17] J. Otera, N. Danoh, H. Nozaki, Tetrahedron 48 (1992) 1449.
[18] J. Otera, Chem. Rev. 93 (1993) 1449.
[19] S. Roelens, J. Org. Chem. 61 (1996) 5257.
[20] A. Morcuende, M. Ors, S. Valverde, B. Herradon, J. Org. Chem. 61 (1996) 5264.
[21] J. Otera, K. Kawada, T. Yano, Chem. Lett. (1996) 225.
[22] A. Orita, A. Mitsutome, J. Otera, J. Org. Chem. 63 (1998) 2420.
[23] A. Orita, K. Sakamoto, Y. Hamada, A. Mitsutome, J. Otera, Tetrahedron 55 (1999) 2899.
[24] Y. Hori, T. Hagiwara, Int. J. Biol. Macromol. 25 (1999) 237.
[25] J. Xiang, S. Toyoshima, A. Orita, J. Otera, Angew. Chem. Int. Ed. Engl. 40 (2001) 3670.
[26] J.D. Murray, C.K. Chu, J. Chem. Soc. A. (1971) 360.
[27] P.G. Harrison, M.J. Begley, K.C. Molloy, J. Organomet. Chem. 186 (1980) 213.
[28] H. Puff, E. Friedrichs, F. Visel, Z. Anorg. Allg. Chem. 477 (1981) 50.
[29] H. Puff, I. Bung, E. Friedrichs, A. Jansen, J. Organomet. Chem. 254 (1983) 23.
[30] J.F. Vollano, R.O. Day, R.R. Holmes, Organometallics 3 (1984) 745.
[31] R. Hämäläinen, U. Turpeinen, J. Organomet. Chem. 333 (1987) 323.
[32] H. Reuter, R. Pawlak, Acta Crystallogr. Sect. C 56 (2000) 804.
[33] A.G. Davies, P.G. Harrison, P.R. Palan, J. Chem. Soc. C (1970) 2030.
[34] D. Dakternieks, K. Jurkschat, S. van Dreumel, E.R.T. Tiekink, Inorg. Chem. 36 (1997) 2023.
[35] J. Beckmann, M. Biesemans, K. Hassler, K. Jurkschat, J.C. Martins, M. Schurmann, R. Willem, Inorg. Chem. 37 (1998) 4891.
[36] K.C. Pande, J. Organomet. Chem. 13 (1968) 187.
[37] V.K. Jain, V.B. Mokal, P. Sandor, Magn. Reson. Chem. 30 (1992) 1158.
[38] I.A. Ahmed, G. Kastner, H. Reuter, D. Schultze, J. Organomet. Chem. 649 (2002) 147.
[39] D. Tudela, J. Organomet. Chem. 471 (1994) 63.
[40] D. Dakternieks, K. Jurkschat, E.R.T. Tiekink, Main Group Met. Chem. 17 (1994) 471.
[41] R.K. Ingham, S.D. Rosenberg, H. Gilman, Chem. Rev. 60 (1960) 459.
[42] T. Yano, K. Nakashima, J. Otera, R. Okawara, Organometallics 4 (1985) 1501.
[43] D.C. Gross, Inorg. Chem. 28 (1989) 2355.
[44] R.K. Harris, A. Sebald, D. Furlani, G. Tagliavini, Organometallics 7 (1988) 388.
[45] D. Dakternieks, F.S. Kuan, E.R.T. Tiekink, Main Group Met. Chem. 24 (2001) 291.
[46] D.L. Tierney, P.J. Moehs, D.L. Hasha, J. Organomet. Chem. 620 (2001) 211.
[47] D.L. Hasha, J. Organomet. Chem. 620 (2001) 296.
[48] J. Beckmann, M. Henn, K. Jurkschat, M. Schürmann, D. Dakternieks, A. Duthie, Organometallics 21 (2002) 192.
[49] T.P. Lockhart, W.F. Manders, E.M. Holt, J. Am. Chem. Soc. 108 (1986) 6611.
[50] E.R.T. Tiekink, Appl. Organomet. Chem. 5 (1991) 1.
[51] E.R.T. Tiekink, Trends Organomet. Chem. 1 (1994) 71.
[52] I.A. Ahmed, H. Reuter, G. Kastner, Z. Kristallogr. 217 (2002) 107.
[53] N. Walker, D. Stuart, Acta Crystallogr. Sect. A 39 (1983) 158.
[54] SADABS (Version 2.01), Bruker AXS Inc, Madison, WI, 2000.
[55] P.T. Beurskens, G. Admiraal, G. Beurskens, W.P. Bosman, S. García-Granda, J.M.M. Smits, C. Smykalla, The DIRDIF program system, Technical Report of the Crystallography Laboratory, University of Nijmegen, The Netherlands, 1994.
[56] G.M. Sheldrick, SHELX-97. Program for the Refinement of Crystal Structures, University of Göttingen, Germany, 1997.
[57] H.D. Flack, Acta Crystallogr. Sect. A 39 (1983) 876.
[58] C.K. Johnson, ORTEP-II, Report ORNL-5138, Oak Ridge National Laboratory, Oak Ridge, TN, 1976.
[59] TEXSAN, Structure Analysis Package, Molecular Structure Corporation, Woodlands, TX, 1992.